Journal of Applied Research in Water and Wastewater
E - ISSN: 2476-6283
Journal homepage: https://arww.razi.ac.ir

The enhancement in dye removal and antifouling capability of PES nanofiltration membrane modified with fumarate-alumoxane nanoparticles

Golshan Moradi[1], Sirus Zinadini[2,*], Masoud Rahimi[*,1]

[1]CFD Research Centre, Department of Chemical Engineering, Faculty of Engineering, Razi University, Kermanshah, Iran.
[2]Environmental Research Center, Department of Applied Chemistry, Razi University, Kermanshah, Iran.

GRAPHICAL ABSTRACT

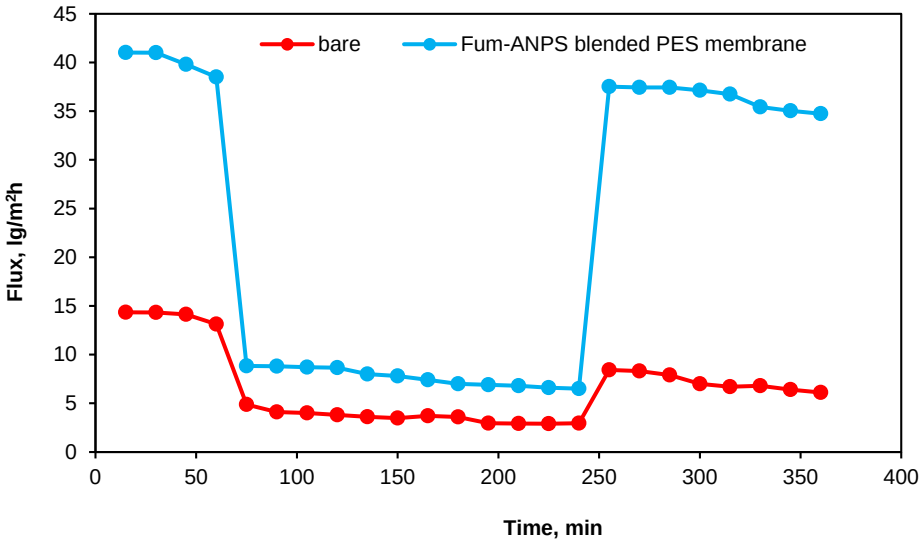

ARTICLE INFO

Article type:
Research Article

Article history:
Received 6 March 2025
Received in revised form 11 May 2025
Accepted 13 May 2025
Available online 30 June 2025

Keywords:
Nanofiltration
Polyethersulfone
Antifouling
Fumarate-alumoxane nanoparticles
Dye removal

ABSTRACT

Fumarate-alumoxane nanoparticles (Fum-ANPs) incorporated PES nanofiltration membrane was fabricated via phase inversion to achieve favorable performance as the enhancement in the dye removal and antifouling capacity. FTIR spectra of the Fum-ANPs revealed that the carboxylate and hydroxyl functional groups were created on the surface of Fum-ANPs. The strong affinity of Fum-ANPs functional groups with water molecules made the membrane surface more hydrophilic. Hence, the modified membrane sample had a higher pure water flux than the bare one. Zeta potential data showed that the Fum-ANPs blended PES membrane was negatively charged at a pH value of 6, which is favorable for negatively charged solute rejection. The antifouling behavior of the membranes was analyzed using powder milk solution (8 g/L) in a dead-end filtration system. The obtained results demonstrated that the introduction of Fum-ANPs in the membrane matrix ameliorated the antifouling behavior of the resulting membrane. To further study the performance of the Fum-ANPs incorporated PES membrane, removal of Direct red 16 dye was tested. The removal efficiency of Direct red 16 with the Fum-ANPs blended PES membrane was 99% while it was 88.2% for the bare membrane sample.

1. Introduction

Water scarcity has become a great menace owing to rapid population and industrialization growth worldwide (Moradi *et al*., 2018a). Among various water purification procedures, membrane filtration technology is increasingly used for wastewater treatment due to its low cost, simple equipment, small-size footprint, and high separation efficiency (W. Wang *et al*., 2018). For example, nanofiltration (NF) membranes are widely applied for the rejection of contaminations with a molecular weight of 100-1000 Da (Ji *et al*., 2012). NF membranes have been widely studied as antifouling membranes as well (Cheng *et al*., 2012). Polyethersulfone (PES) has been increasingly used for polymeric membrane fabrication owing to excellent advantages such as high stiffness, good dimensional stability, high level of molecular immovability providing creep resistance, and excellent mechanical strength (Rahimpour and Madaeni, 2007). However, there still remains a limitation (hydrophobicity) for the practical application of

*Corresponding author Email: sirus.zeinaddini@gmail.com

Cite this article: G. Moradi, S. Zinadini, M. Rahimi, The enhancement in dye removal and antifouling capability of PES nanofiltration membrane modified with fumarate-alumoxane nanoparticles, *Journal of Applied Research in Water and Wastewater*, 12 (1), 2025, 1-6. doi: https://doi.org/10.22126/arww.2020.5646.1185

PES membrane in wastewater treatment (Rahimpour and Madaeni, 2007). Several methods like grafting with hydrophilic monomer, plasma treatment, hydrophilic coating, and blending with hydrophilic nanoparticles have been suggested to improve the hydrophilicity of PES membranes (Zinadini *et al*., 2014). Blending nanoparticles possessing hydrophilicity, good thermal, and chemical stability into the membrane matrix is among the promising way to improve surface hydrophilicity and antifouling properties (Moradi *et al*., 2018a). Up to now, several nanofiillers such as Fe_3O_4, multiwalled carbon nanotubes, boehmite, graphene oxide, metal-organic frameworks, TiO_2 were blended into PES membranes (Zangeneh *et al*., 2019). Zinadini *et al*. fabricated the PES membranes blended with ZnO-multi walled carbon nanotubes with enhanced antifouling characteristics and dye rejection (Zinadini *et al*., 2017). A previous study demonstrated the effect of boehmite nanoparticles in improving the hydrophilicity and antifouling characteristics of PES membranes (Vatanpour *et al*., 2012). On the other hand, the addition of boehmite nanoparticles into the membrane matrix affected the surface morphology, roughness/smoothness, and the structure of the membrane resulted in improving surface hydrophilicity (X. Wang *et al*., 2018). Fumare-Alumoxane nanoparticles (Fum-ANPs) are fumaric acid functionalized boehmite nanoparticles which can be prevalent candidates for membrane fabrication (Moradi *et al*., 2018b). This is due to their high hydrophilicity and specific surface area. In our previous work, we fabricated Fum-ANPs embedded polyacrylonitrile nanofibrous membrane via electrospinning (Moradi *et al*., 2018b). The prepared membranes exhibited good antifouling properties. Herein, the Fum-ANPs incorporated PES membrane was fabricated via phase inversion method. The antifouling properties and separation performance of the Fum-ANPs incorporated PES membrane were tested in dead-end filtration apparatus. A series of analysis such as FESEM, FTIR, zeta potential, water contact angle and porosity measurements were used to characterization the Fum-ANPs and the Fum-ANPs incorporated PES membrane.

2. Materials and methods

2.1. Materials

Aluminum nitrate, fumaric acid, and sodium hydroxide were provided from Merck. Polyethersulfone with a molecular weight of 58,000 g/mol (polymer) and dimethylacetamide (DMAc-solvent) was purchased from BASF Co. (Germany). Polyvinyl pyrrolidone (PVP) with a molecular weight of 25,000 g/mol was obtained from Mowiol (Germany). Distilled water and ethanol were utilized during this study.

2.2. Fabrication of the Fum-ANPs blended PES membrane

The Fum-ANPs were synthesized via the method we explained elsewhere (Moradi *et al*., 2018b). 0.5 wt.% Fum-ANPs and 1 wt.% PVP (pore-forming agent) was first added to DMAc under ultrasound mixing for half an hour. 1 h sonication followed by 12 h stirring was carried out to dissolving 20 wt.% PES in DMAc-NPs solution. The resulting solution was then kept in an oven at 30˚C for 4 h to remove bubbles as possible. Next, each solution was poured in a 15×20 clean glass plate using a film casting knife (thickness=200 µm) and the plate was immediately immersed in deionized water bath for about 2 min. Afterward, the resulting membranes were stored in deionized water and then dried at room temperature for 1 day. The bare membrane fabrication method was similar to the fabrication procedure described for the Fum-ANPs incorporated PES membrane (FU-0.5) expect that the Fum-ANPs were not used.

2.3. Characterization

FTIR spectrum was analyzed by Bruker FTIR spectrophotometer within the confines of 400–4000 cm^{-1}. The structure of the Fum-ANPs and the Fum-ANPs incorporated PES membrane was inspected using a field emission scanning electron microscopy (FESEM, CamScan MV2300). The measurement of water contact angle (WCA) with the Fum-ANPs incorporated PES membrane was carried out with a 3µL deionized water droplet with a CCD camera (Dataphysics OCA 15 plus contact angle analysis system, Germany). At least six spots at random locations on the sample were measured, and the average value was reported to get reliable data. The overall porosity was calculated using the gravimetric method according to equation 1, in which ε is overall porosity, ρ denotes the density of water, A denotes the membrane available area, and L denotes the membrane thickness. W_{wet} and W_{dry} refer to the weight of wet and dry membranes, respectively.

$$\varepsilon(\%)=(w_{wet}-w_{dry})/\rho.A.L \quad (1)$$

2. Membrane performance

The separation performance of the samples was examined in stainless steel dead-end filtration unit with the available membrane area and volume of 12.56 cm^2 and 0.2 L, respectively. Before measuring the permeate flux, each membrane sample was first compacted with deionized water at a transmembrane pressure of 5 bar for 25 min at room temperature. After pre-compacting the membrane samples with deionized water, the pure water flux ($F(L/m^2h)$) was measured according to Eq. 2.

$$F(L/m^2h)=V/A.\Delta t \quad (2)$$

where V, A, and Δt refer to the permeate volume, available area of the membrane, and filtration time, respectively.

The antifouling properties of the samples were investigated through the following procedure. After the pure water flux measuring, the permeation flux of powder milk solution ($F_p(L/m^2h)$) was measured using the filtration of powder milk solution (8000 ppm) for 3 h, and the volume of permeate was measured each 15 min. Afterward, physical cleaning of membrane samples with deionized water was performed for 15 min, and the permeate flux of deionized water ($F_1(L/m^2h)$) was measured again. The operating pressure was set to 4 bar during whole experiments. Then, the flux recovery ratio (FRR) and three fouling resistance indexes including total fouling ratio (R_t), reversible fouling ratio (R_r), and irreversible fouling ratio (R_{ir}) were calculated using Eqs. 3-6 (Rahimi *et al*., 2014).

$$FRR=(F_1/F)\times100 \quad (3)$$

$$R_t=(1-F_p/F) \quad (4)$$

$$R_r=(F_1-F_p/F)\times100 \quad (5)$$

$$R_{ir}=(F-F_1/F)\times100 \quad (6)$$

The nanofiltration performance of the Fum-ANPs blended PES membrane was studied through rejection of Direct red 16 dye. The initial and final concentration of dye in feed and permeate sides were determined using UV-2450 model UV-VIS spectrophotometer (Shimadzu, Japan) at λ_{max} of 526 nm, and the dye rejection was calculated by:

$$R(\%)=(C_f-C_p).100/C_f \quad (7)$$

3. Results and discussion

3.1. Characterization of Fum-ANPs

Agglomeration of small-size Fum-ANPs is shown in FESEM image (Fig. 1). FTIR measurement was carried out to elucidate the chemical compositions of Fum-ANPs. As seen in Fig. 1, the peaks at 1608 and 1426 were ascribed to the carboxylate bonds. The peak appears around 1158 was related to the symmetric hydrogen bond between hydroxyl groups. The peak at 3438 corresponded to hydroxyl groups.

3.2. Analysis of morphology, zeta potential and overall porosity

To study the effects of the Fum-ANPs on the structure of the bare and FU-0.5 membranes, cross-sectional FESEM pictures of these membrane samples were made (Fig. 2). Both membranes had a similar anisotropic structure with a thin, compact top layer on a macroporous substructure, representing that the introduction of the Fum-ANPs did not considerably change the morphologies of cross-section.

Zeta potential is used as an effectual tool to indicate the charge of the membrane. Zeta potential data at pH=6 for the bare and FU-0.5 membranes are displayed in Fig. 3. Both the bare and FU-0.5 membranes were negatively charged at a pH value of 6, which is favorable for negatively charged solute rejection. In the presence of the Fum-ANPs, the negative charge of membrane surface increased owing to the presence of hydroxyl and carboxylate groups on the surface of FU-0.5 membrane sample. The de-protonation of hydroxyl and carboxylate groups in hydrous media was the cause of an increase in the negative charge.

It is worth mentioning that the overall porosity of the bare membrane sample increase from 73.5 to 85% along with the introduction of the Fum-ANPs (Fig. 4.). In fact, the kinetic and thermodynamic of the system during phase inversion are the most important factors that exert influences on the final morphology of the membrane (Moradi *et al*., 2020b).

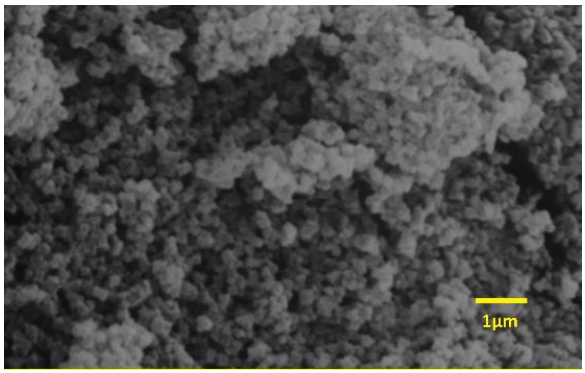

(a)

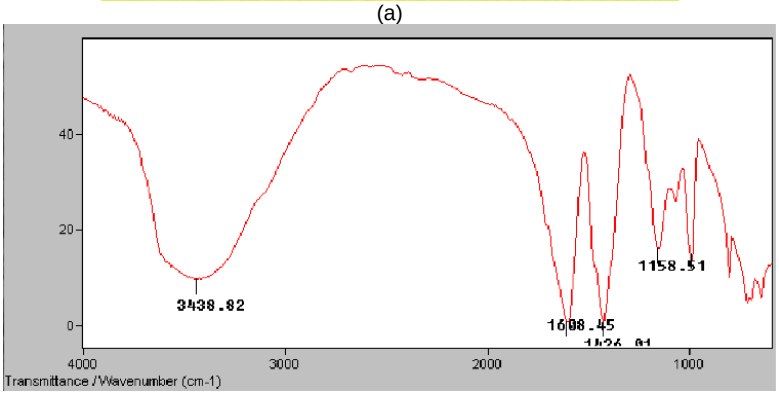

(b)

Fig. 1. SEM image and FTIR spectrum of Fum-ANPs.

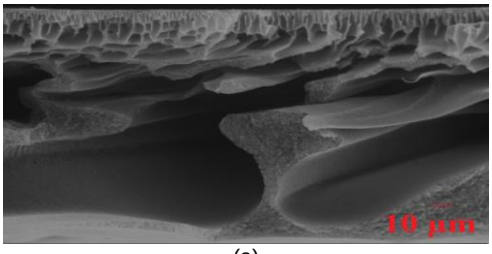

(a)

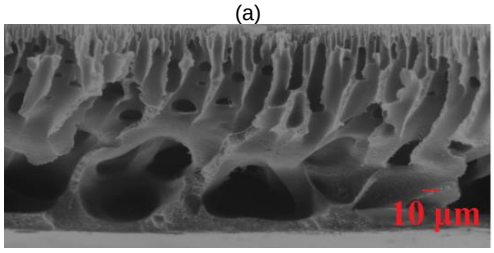

(b)

Fig. 2. The cross-sectional FESEM picture of (a) bare and (b) FU-0.5 membrane samples.

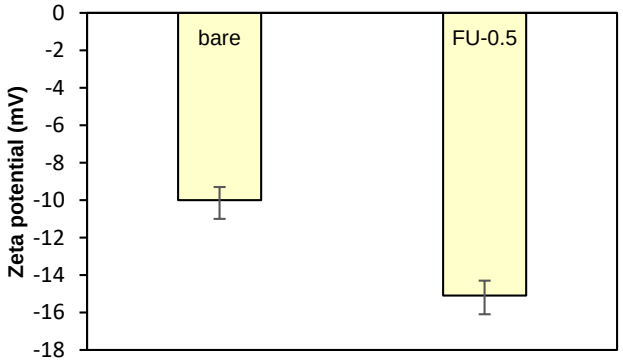

Fig. 3. Zeta potential of the bare and FU-0.5 membrane samples.

Increment in hydrophilicity of casting solution via increasing the rate of mass transfer between water and non-solvent phases during phase inversion can affect these factors (the kinetic and thermodynamic aspects of the system) and alter the final morphology of the fabricated membranes through the formation of pores with larger sizes (Kamari and Shahbazi, 2020). As a result, the Fum-ANPs played a pore causing role and increase the overall porosity of the resulting membrane.

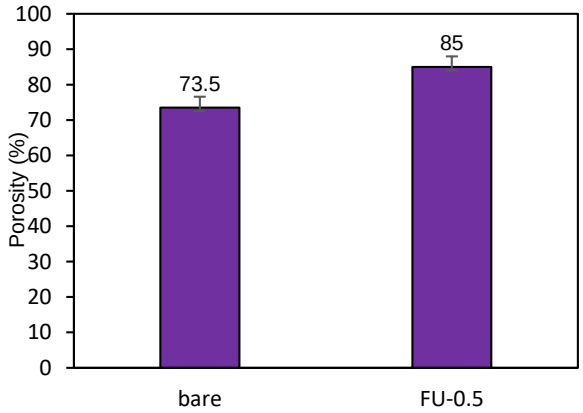

Fig. 4. Overall porosity of the bare and FU-0.5 membrane samples.

3.3. Pure water flux and surface hydrophilicity

The existence of functional groups, as proved by FTIR analysis, remarkably ameliorates the surface hydrophilicity of the Fum-ANPs blended PES membrane. The water contact angle measurements, represented in Fig. 5, also show the hydrophilicity improvement of the PES membrane upon the introduction of Fum-ANPs. As shown, the water contact angle increased for the bare sample from 66±2.1 to 51±2.0° for FU-0.5, representing the hydrophilic quiddity of the Fum-ANPs. On the other hand, the strong affinity of Fum-ANPs functionalities (carboxylate and hydroxyl) with water molecules makes the membrane surface more hydrophilic (Moradi *et al*., 2018a). The enhancement in hydrophilicity plays an important role in increasing permeate flux and improving the antifouling properties of the membrane.

The pure water flux of the bare and FU-0.5 membranes was also tested for comparison, and the related results are shown in Fig. 5. It is clearly understood that the FU-0.5 membrane sample had a higher pure water flux than the bare one. Hydrophilicity and porosity increase are the principal motives for the increase in pure water flux. As the surface porosity increase, water molecules are more allowed to pass across the membrane which causes an increment of pure water flux (Moradi *et al*., 2020a).

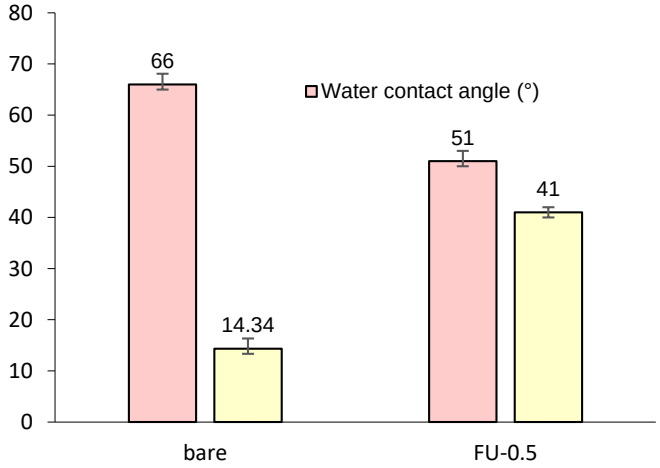

Fig. 5. The water contact angle and pure water flux of the bare and FU-0.5 membrane samples.

3.4. Antifouling analysis

Fouling is considered as the main disadvantageous of the membrane which increases the flux decline, operational, and maintenance cost. Up to now, many attempts consisting of plasma treatment, surface modification, blend with other polymers, fillers, and nanofillers have been made to ameliorate the antifouling behavior of membranes (Oulad *et al*., 2019). Blending of nanoparticles possessing hydrophilicity, good thermal, and chemical stability into the membrane matrix is among the promising way to ameliorate surface hydrophilicity and antifouling behavior (Moradi *et al*., 2018b).

In order to study the antifouling behavior of the membranes, powder milk solution (8 g/L) were analyzed using a dead-end filtration apparatus. Flux alteration for the bare and FU-0.5 membrane samples during filtration of powder milk solution and alternative pure water flux is shown in Fig. 6. As shown, the FU-0.5 had higher permeation flux for powder milk solution than the bare membrane, which emphasizing the prevalent effect of the Fum-ANPs on antifouling behavior. The calculated FRR data, as the most important fouling parameter, clearly demonstrate that the introduction of Fum-ANPs in the membrane matrix ameliorated the antifouling behavior of the resulting membrane. The FRR of FU-0.5 membrane measured 91.48% which was higher than the bare one (58.61%). Water molecules are more allowed to adsorbed on the membrane with higher surface hydrophilicity; these accumulated water molecules act as a hindrance layer against foulants deposition on the membrane surface (Moradi *et al*., 2020b).

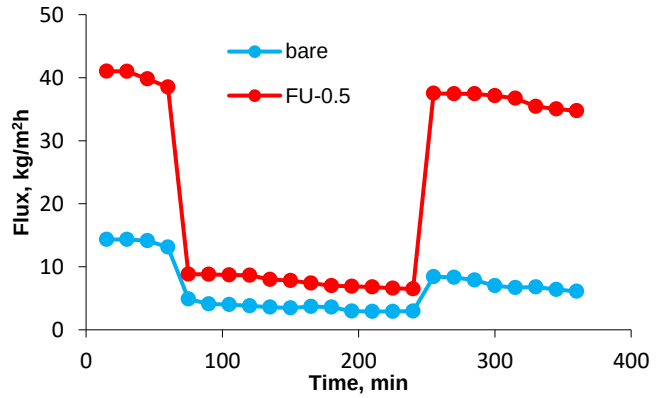

Fig. 6. Permeation flux against time during 0-60 min, 60-240 min, and 240-360 min filtration of distilled water, powder milk solution, and distilled water for the bare and FU-0.5 membrane samples at a transmembrane pressure of 4 bar.

In general, fouling can be classified into irreversible fouling and reversible fouling. Frail sticking of foulant on the membrane surface constitutes the reversible fouling which can be eliminated through hydraulic cleaning. However, entrapment of foulants within the membrane pores or strong adsorption of them on the membrane surface constitutes the irreversible fouling which can be wiped out only through chemical cleaning methods (Oulad *et al*., 2019). Fig. 8 shows these fouling parameters for the bare and FU-0.5 membrane samples. This was due to the lower deposition of foulants on the FU-0.5 with higher surface hydrophilicity.

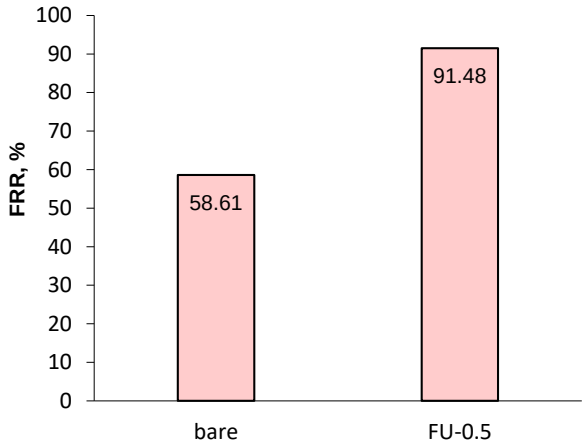

Fig. 7. FRR (%) of the bare and FU-0.5 membrane samples.

Despite the simple adsorption of biomolecules like proteins onto the hydrophobic surface towards reducing surface energy, the hydrophilic surface can efficiently withstand the adherence and deposition of proteins due to its low top layer-water interfacial energy (Pirsaheb *et al*., 2019).

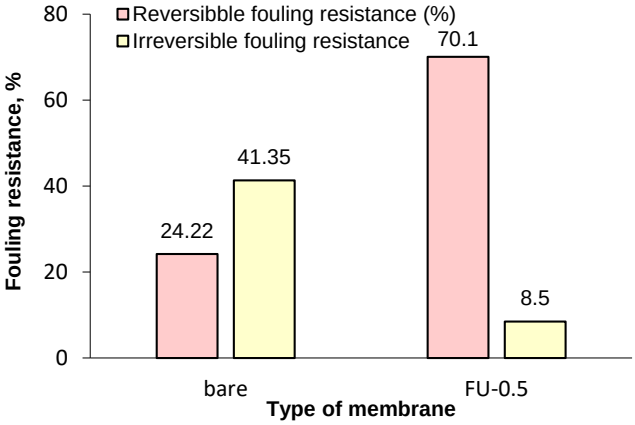

Fig. 8. Reversible and irreversible fouling resistance (%) of the bare and FU-0.5 membrane samples.

3.5. Direct red 16 removal

The nanofiltration performance of the Fum-ANPs incorporated PES membrane was studied by the rejection of Direct red 16 dye. Dye removal tests were carried out under a fixed feed dye concentration of 30 mg/l using a handmade dead-end filtration apparatus at a transmembrane pressure of 4 bar and solution pH of 6. The calculated rejection data are illustrated in Fig. 9 and the permeation flux of testing dye solution for testing membranes after 1 h filtration is illustrated in Fig. 10.

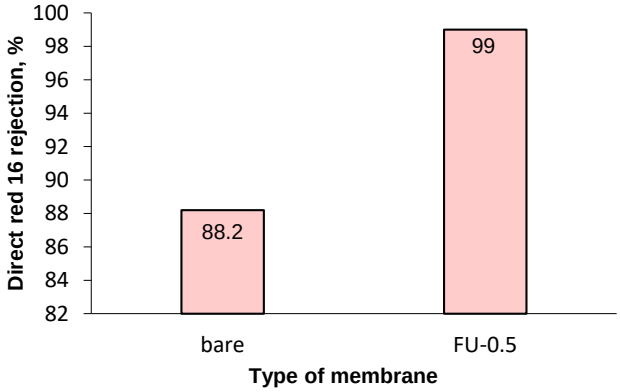

Fig. 9. Direct red 16 dye rejection of the bare and FU-0.5 membrane samples.

From these figures, the Direct red 16 rejection with FU-0.5 was 99% while it was 88.2% for the bare membrane sample. As zeta potential data in Fig. 3 suggests, the FU-0.5 had a more negative charge than the bare one. Hence, more negatively charged Direct red

16 dye molecules were rejected using FU-0.5 sample with higher negative surface charged through the Donnan exclusion effect. Compared with the pure water flux of the bare and FU-0.5 membrane sample (Fig. 5), the dye solution permeation flux of these membranes was slightly lower, this slight reduction in permeation flux may be related to fouling phenomenon in the presence of Direct red 16 molecules. However, the dye solution permeation flux of the FU-0.5 membrane sample was higher due to its superior antifouling behavior (Figs. 6-8).

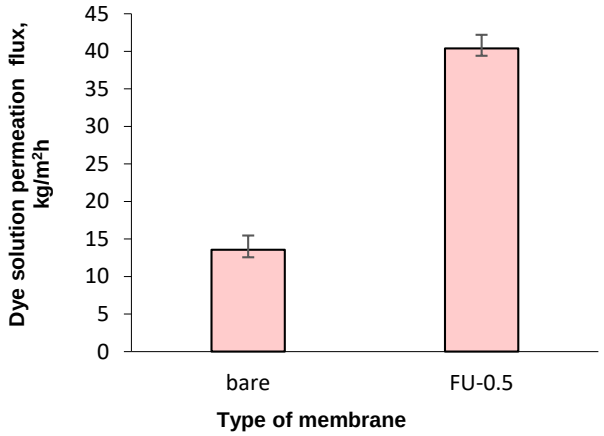

Fig. 10. Dye solution permeation flux of the bare and FU-0.5 membrane samples.

4. Conclusions

Nanofiltration membrane consisting of Fumarate-Alumoxane nanoparticles (Fum-ANPs) and polyethersulfone (PES) was fabricated via phase inversion method and used as an antifouling membrane. Agglomeration of small-size Fum-ANPs was shown in SEM analysis. The FTIR spectrum of the Fum-ANPs revealed that the desired functional groups were successfully created on the surface of Fum-ANPs. FESEM analysis showed that both bare and the Fum-ANPs incorporated PES nanofiltration membranes had a similar anisotropic structure with a thin, compact top layer on a macroporous substructure, representing that the introduction of the Fum-ANPs did not considerably change the morphologies of the cross-section. The overall porosity of the bare membrane sample increase from 73.5 to 85% along with the introduction of the Fum-ANPs. The effects of the Fum-ANPs on pure water flux, surface hydrophilicity, antifouling behavior, and dye removal were studied. The water contact angle increased for a bare sample from 66±2.1 to 51±2.0° for the Fum-ANPs incorporated PES membrane, representing the hydrophilic quiddity of the Fum-ANPs. The Fum-ANPs incorporated PES membrane had higher permeation flux and antifouling properties than bare membrane which emphasizing the prevalent effect of the Fum-ANPs on antifouling behavior. Moreover, the Direct red 16 rejection with the Fum-ANPs incorporated PES membrane was 99% while it was 88.2% for the bare membrane sample.

Author Contributions

Golshan Moradi: Conceived and designed the analysis, Collected the data, Contributed data or analysis tools, Performed the analysis, Wrote the paper
Sirus Zinadini: Conceived and designed the analysis, Contributed data or analysis tools
Masoud Rahimi: Conceived and designed the analysis, Contributed data or analysis tools

Data Availability Statement

The data would be available on the request.

Acknowledgment

The authors wish to thank Razi University, Iran, for the equipped lab.

Conflict of Interest

The authors have no conflict of interest.

References

Cheng, S., Oatley, D.L., Williams, P.M., Wright, C.J., 2012. Characterisation and application of a novel positively charged nanofiltration membrane for the treatment of textile industry wastewaters. Water Res. 46, 33–42. https://doi.org/10.1016/j.watres.2011.10.011

Ji, Y.L., An, Q.F., Zhao, Q., Sun, W.D., Lee, K.R., Chen, H.L., Gao, C.J., 2012. Novel composite nanofiltration membranes containing zwitterions with high permeate flux and improved anti-fouling performance. J. Memb. Sci. 390–391, 243–253. https://doi.org/10.1016/j.memsci.2011.11.047

Kamari, S., Shahbazi, A., 2020. Biocompatible Fe3O4@SiO2-NH2 nanocomposite as a green nanofiller embedded in PES–nanofiltration membrane matrix for salts, heavy metal ion and dye removal: Long–term operation and reusability tests. Chemosphere 243, 125282. https://doi.org/10.1016/j.chemosphere.2019.125282

Moradi, G., Dabirian, F., Mohammadi, P., Rajabi, L., Babaei, M., Shiri, N., 2018a. Electrospun fumarate ferroxane/polyacrylonitrile nanocomposite nanofibers adsorbent for lead removal from aqueous solution: Characterization and process optimization by response surface methodology. Chem. Eng. Res. Des. 129, 182–196. https://doi.org/10.1016/j.cherd.2017.09.022

Moradi, G., Zinadini, S., Rajabi, L., 2020a. Development of high flux nanofiltration membrane using para-amino benzoate ferroxane nanoparticle for enhanced antifouling behavior and dye removal. Process Saf. Environ. Prot. 144, 65–78. https://doi.org/10.1016/j.psep.2020.06.044

Moradi, G., Zinadini, S., Rajabi, L., Ashraf Derakhshan, A., 2020b. Removal of heavy metal ions using a new high performance nanofiltration membrane modified with curcumin boehmite nanoparticles. Chem. Eng. J. 390, 124546. https://doi.org/10.1016/j.cej.2020.124546

Moradi, G., Zinadini, S., Rajabi, L., Dadari, S., 2018b. Fabrication of high flux and antifouling mixed matrix fumarate-alumoxane/PAN membranes via electrospinning for application in membrane bioreactors. Appl. Surf. Sci. 427, 830–842. https://doi.org/10.1016/j.apsusc.2017.09.039

Oulad, F., Zinadini, S., Zinatizadeh, A.A., Derakhshan, A.A., 2019. Influence of process and operating variables on the performance and fouling behavior of modified nanofiltration membranes treating licorice aqueous solution. J. Appl. Res. Water Wastewater 12, 131–137. https://arww.razi.ac.ir/article_1412.html

Pirsaheb, M., Hossein Davood Abadi Farahani, M., Zinadini, S., Zinatizadeh, A.A., Rahimi, M., Vatanpour, V., 2019. Fabrication of high-performance antibiofouling ultrafiltration membranes with potential application in membrane bioreactors (MBRs) comprising polyethersulfone (PES) and polycitrate-Alumoxane (PC-A). Sep. Purif. Technol. 211, 618–627. https://doi.org/10.1016/j.seppur.2018.10.041

Rahimi, Z., Zinatizadeh, A.A., Zinadini, S., 2014. Preparation and characterization of a high antibiofouling ultrafiltration PES membrane using OCMCS-Fe3O4 for application in MBR treating wastewater. J. Appl. Res. Water Wastewater 1, 13–17. https://arww.razi.ac.ir/article_45.html

Rahimpour, A., Madaeni, S.S., 2007. Polyethersulfone (PES)/cellulose acetate phthalate (CAP) blend ultrafiltration membranes: Preparation, morphology, performance and antifouling properties. J. Memb. Sci. 305, 299–312. https://doi.org/10.1016/j.memsci.2007.08.030

Vatanpour, V., Madaeni, S.S., Rajabi, L., Zinadini, S., Derakhshan, A.A., 2012. Boehmite nanoparticles as a new nanofiller for preparation of antifouling mixed matrix membranes. J. Memb. Sci. 401–402, 132–143. https://doi.org/10.1016/j.memsci.2012.01.040

Wang, W., Zhu, L., Shan, B., Xie, C., Liu, C., Cui, F., Li, G., 2018. Preparation and characterization of SLS-CNT/PES ultrafiltration membrane with antifouling and antibacterial properties. J. Memb. Sci. 548, 459–469. https://doi.org/10.1016/j.memsci.2017.11.046

Wang, X., Wang, T., Ma, J., Liu, H., Ning, P., 2018. Synthesis and characterization of a new hydrophilic boehmite-PVB/PVDF blended membrane supported nano zero-valent iron for removal of Cr(VI). Sep. Purif. Technol. 205, 74–83. https://doi.org/10.1016/j.seppur.2018.05.010

Zangeneh, H., Zinatizadeh, A.A., Zinadini, S., Feyzi, M., Bahnemann, D.W., 2019. Preparation and characterization of a novel

photocatalytic self-cleaning PES nanofiltration membrane by embedding a visible-driven photocatalyst boron doped-TiO2–SiO2/CoFe2O4 nanoparticles. Sep. Purif. Technol. 209, 764–775. https://doi.org/10.1016/j.seppur.2018.09.030

Zinadini, S., Rostami, S., Vatanpour, V., Jalilian, E., 2017. Preparation of antibiofouling polyethersulfone mixed matrix NF membrane using photocatalytic activity of ZnO/MWCNTs nanocomposite. J. Memb. Sci. 529, 133–141. https://doi.org/10.1016/j.memsci.2017.01.047

Zinadini, S., Zinatizadeh, A.A., Rahimi, M., Vatanpour, V., Zangeneh, H., 2014. Preparation of a novel antifouling mixed matrix PES membrane by embedding graphene oxide nanoplates. J. Memb. Sci. 453, 292–301. https://doi.org/10.1016/j.memsci.2013.10.070